Nigerian Journal of Technology (NIJOTECH)
Vol. 39, No. 1, January 2020, pp. **161 – 172**

Print ISSN: 0331-8443, Electronic ISSN: 2467-8821
www.nijotech.com
http://dx.doi.org/10.4314/njt.v39i1.18

A 3D MODELLING OF THE IN-CYLINDER COMBUSTION DYNAMICS OF TWO STROKE INTERNAL COMBUSTION ENGINE IN ITS SERVICE CONDITION

A. E. Ikpe [1],* and I. B. Owunna[2]
[1, 2], DEPARTMENT OF MECHANICAL ENGINEERING, UNIVERSITY OF BENIN, BENIN CITY, EDO STATE, NIGERIA
E-mail addresses: [1] *aniekan.ikpe@eng.uniben.edu,* [2] *ikechukwu.owunna@uniben.edu*

ABSTRACT
In this study, a two stroke internal combustion engine was successfully modeled as a closed cycle with the intake, compression, expansion and exhaust processes considered in two strokes of the reciprocating piston. The in-cylinder combusted gases with respect to air-fuel mixture of 14.4:1 in the two stroke engine model were analyzed, showing the dynamics of the combusted gases, the flame pressure and temperature trajectories. It was observed that provided compression and expansion takes place at air-fuel mixture near ideal condition (14.7:1), the combusted gas temperature which occurred in the range of 293.92-3000.60 K is directly proportional to the cylinder gas pressure which occurred in the range of 60.76-80.20 bar. With a heat transfer coefficient of 581.236 W/m^{2}K, the maximum temperature of the IC engine material was found to be 2367.56K at equilibrium and the maximum shear stress was found to be 176 x 10^2 MPa (1.76 x 10^5 bar). The 14.4:1 air-fuel mixture implies that 26% O_2, 73% N_2 and 1% trace gases are the in-cylinder air constituent that will react with 1 mole of hydrocarbon to form the combusted products of 96.2% CO_2, 3.2% H_2O and 0.6% N_2. This will vary in conditions where the air-fuel mixture changes.

Keywords: *Modelling, Gas dynamics, Two stroke, IC engine, Air-fuel mixture.*

1. INTRODUCTION

Internal combustion engines have undergone several improvements over the years, and this has led to relatively low initial cost, high power density and efficiency, ability to meet emission standards as well as compatibility with available fuel options [1]. The combustion of air-fuel mixture in internal combustion engine occurs in the combustion chamber of the engine where mechanical work is achieved. The heat generated in the process reacts with the mixture inside the cylinder to form hot gases, thus increasing the internal pressure within the engine cylinder [2, 3]. The pressurised mixture gradually builds momentum within the cylinder, causing reciprocating movement of the piston which is translated to the rotating motion of the crankshaft [4, 5]. According to Kosenok et al. [6], transformation of the gas energy to mechanical work in the engine cylinder is accompanied by big losses on friction and increased load of supporting bearing resulting from the kinematics of the piston. During the high temperature and pressure expansion of gases in the combustion chamber, discharging of burned gases and recharging of the cylinder with fresh air takes place in the same stroke, and occurs towards the end of the expansion process [7, 8]. The upward motion of the piston within the engine cylinder indicates compression process while the downward motion of the piston indicates the expansion process of the combusted gases [9]. In two stroke internal combustion engine, the entire sequence of operation (suction, compression, power and exhaust) are completed in one revolution of the crankshaft which is two reciprocating strokes of the piston. This type of engine do not have valves, and air intake into the combustion chamber as well as expulsion of combusted gases are accomplished via holes referred to as ports in the cylinder. The opening and closing

* Corresponding author, tel: +234 902 477 3812

of the ports are performed by the piston motion [10]. The combusted air-fuel mixture in the cylinder contain many elements but the atoms are arranged into groups having different chemical properties [11]. For the combustion process, the most important fuel elements are carbon and hydrogen, and most fuels consist of these and sometimes a small amount of sulphur. The fuel may also contain some oxygen and little amount of incombustibles such as water vapour, nitrogen, ash etc. [12, 13]. Compared to four stroke engines, two stroke engines offer some advantages such as low cost, lighter weight, higher specific power, higher speed, ease of maintenance, ability to perform optimally at different working positions. It also has some disadvantages which include relatively low thermodynamic efficiency, higher HC and CO emissions and toxic pollutants, low service life, specific lubricant requirement etc. [14-16].

In combined thermodynamic analysis, the force exerted on the piston by the gases is calculated simultaneously with the other forces and moments involved by the analysis. For calculation of the force, first law of thermodynamics applicable to closed systems is used [17]. Zhang and Assanis [18] numerically computed a one-dimensional unsteady gas dynamics in intake and exhaust manifold as well as with single cylinder engines. It was observed that thermodynamic simulation cycle using uniform pressure, intake and exhaust plenums and quasi-steady state assumptions for the gas exchange process can introduce significant error in both the magnitude and trend of computed volumetric efficiency and Break Mean Effective Pressure (BMEP) with speed. By employing practically specific values, the combined dynamics and thermodynamic behaviour of two stroke internal combustion engine was determined by Duygu and Halit [8]. Andwari *et al.* [19] investigated the effects of Controlled Auto-Ignition (CAI) combustion in two stroke cycle engine using hot burned gases. The result indicated that hot burned gases in two stroke engine cycle increases the cylinder charge temperature without external heating source, while also advances the start of CAI combustion due to their charged heating effect. This study is focused on the modelling of a two stroke internal combustion engine cycle and the corresponding gas dynamics in its service condition.

2. MATERIALS AND METHODS

As shown in Figure 1, the 2-stroke internal combustion engine was modelled using Solidworks software while the engine specification as well as the materials comprising of the engine model (see Table 1) was selected from internal combustion engine material library embedded in the software. Applying the boundary conditions in Table 2, the engine model was simulated and various gas parameters were computed with respect to its dynamics.

.

Table 1: Materials and Engine Specifications for the Engine Model

Engine specifications		Engine Body Material Properties (Aluminum Alloy-2014-T6)	
Compression ratio (r)	10.3	Elastic modulus	7.24e+010 N/m^2
Expansion coefficient (k)	1.4	Poisson's ratio	0.33
Engine speed (RPM)	3000	Shear modulus	2.8e+010 N/mm^2
Bore (mm)	81	Mass density	2800 Kg/m^3
Mass of piston (Ibs)	1	Tensile Strength	470000000 N/m^2
Ratio of crank to connecting rod length	0.35	Thermal expansion coefficient	2.3e-005 K
Clearance volume (litres)	0.05	Compressive Strength	470000000 N/m^2
Mass of connecting rod (Ibs)	1.75	Yield Strength	415000000 N/m^2
Swept volume (cm^3)	499.5	Thermal Conductivity	155 W/(m.k)

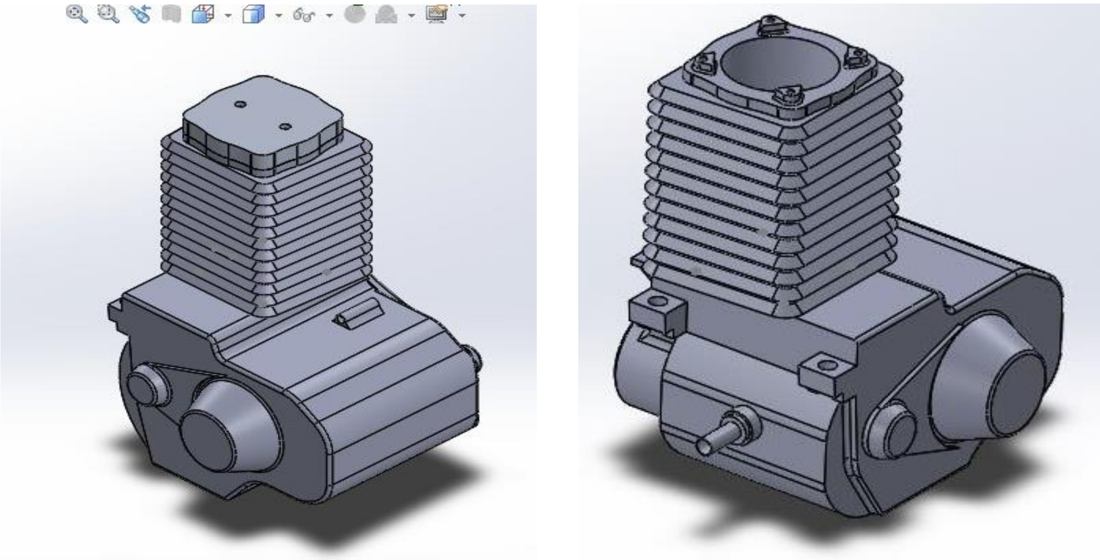

a. Front View b. End View

Fig. 1: Engine Model showing Front and End View

Table 2: Boundary Conditions for the Gas Analysis

Boundary conditions	Values
Thermodynamic parameters	Static Pressure: 1.00 bar Temperature: 298.00 K
Velocity parameters	Velocity vector Velocity in X direction: 20.000 m/s Velocity in Y direction: 10.000 m/s Velocity in Z direction: 15.000 m/s
Solid parameters	Default material: 2014-T6 Initial solid temperature: 293.20 K
Fuel	Gasoline Percent fuel by mass: 6.9%
Flow type	Inlet Mass Flow
Faces	Face<1>@Top Cover-1
Coordinate system	Face Coordinate System
Reference axis	X
Flow parameters	Flow vectors direction: Normal to face Mass flow rate: 0.0020 kg/s Fully developed flow: No Inlet profile: 0
Thermodynamic parameters	Approximate pressure: 7.00 bar Temperature: 298.00 K

3. THERMODYNAMICS OF 2-STROKE IC ENGINE

The two stroke IC engine is a type of heat engine where combusted gases are expelled through the exhaust manifold after intensive high-temperature-high-pressure combustion and expansion of air-fuel mixture in the cylinder. Given by Equation (1), the ratio of the total volume (V_m) of the combustion chamber when the piston is at BDC to the clearance volume when the piston is at TDC is known as compression ratio [20];

$$R_c = \frac{V_c + \left(\frac{\pi}{4} b^2 s\right)}{V_c} \tag{1}$$

Where, V_c is the clearance volume, b is the cylinder bore diameter, s is the piston stroke length, V_m is the sum of the clearance volume and the displacement volume.

Also in Equation (2a), the cylinder volume can be expressed as a function of the crank angle θ and the ratio of the length of the piston rod to the crank.

Furthermore, the cylinder volume at any crank angle is given by Equation (2b) [21];

$$V = V_c + \frac{V_d}{2}\left(1 + \frac{l}{c} - \cos\theta - \sqrt{\frac{l^2}{c^2} - \sin^2\theta}\right) \quad (2a)$$

$$V(\theta) = V_c\left\{1 + \frac{r-1}{2}\left\{1 - \cos\theta + \frac{1}{\varepsilon}\left[1 - (1 - \varepsilon^2 \sin^2\theta)^{0.5}\right]\right\}\right\} \quad (2b)$$

Where, V_c is the clearance volume, V_d is the displacement volume, r is the compression ratio and ε is the piston stroke given by Equation (2c) [22];

$$\varepsilon = \frac{\text{stroke}}{2 \text{ x length of connecting rod}} \quad (2c)$$

The first law of thermodynamics for the control volume that encloses the combusted gases present in the cylinder is given by the general expression in Equation (3);

$$\frac{dU}{dt} = \overline{f_\iota}\overline{h_\iota} - \overline{f_e}\overline{h_e} + \frac{dQ}{dt} - \frac{dW}{dt} \quad (3)$$

Where, $\overline{f_\iota}$ and $\overline{f_e}$ are the gas flow rates entering or leaving the cylinder, U is the total internal energy of the gases contained in the cylinder, $\overline{h_\iota}$ and $\overline{h_e}$ are the mass specific enthalpies of the gasses entering and exiting the cylinder, *Q* signifies the heat transferred to the gases, *W* is the work done by the gas pressure. In conditions where the cylinder is completely closed with no incoming air or outgoing gases, the energy equation can be given by Equation (4) [23];

$$\frac{d}{dt} = (m\bar{u}_T) = \frac{dQ}{dt} - P\frac{dV}{dt} \quad (4)$$

Where, $\bar{u}_T$ is the total mass specific internal energy in Equation (5), *p dv/dt* is the work done by the gases due to expansion, *Q* is the heat transferred out of the charge and *m* is the total mass of the charge. The average burned gases in the cylinder is given by Equation (6) [24];

$$\bar{u}_T = \alpha\langle\bar{u}_b\rangle + (1-\alpha)\langle\bar{u}_u\rangle \quad (5)$$

$$\langle\bar{u}_b\rangle(\alpha) = \int_0^\alpha \bar{u}_b(\alpha, \alpha')\, d\alpha' \quad (6)$$

Where, $\bar{u}_b$ is the energy when combustion has progressed to burned gas mass fraction α, $\bar{u}_u$ denotes the unburn gas.

Given by Equation (7), the internal energy of burned and unburned gas can be expressed in terms of the specific heat ($\bar{C}_{vi}$) in Equation (8). Internal energies of the burned and unburned gases may be expressed in terms of the average specific heat in Equation (9) and Equation (10).

$$\bar{u}_i = \Delta\bar{u}_{f_i}^{o}(T_o) + \int_{To}^{T} \bar{C}_{vi}(T')dT' \quad (7)$$

$$\bar{C}_{vi} = \frac{\int_{T_1}^{T_2}(a_i + b_i T)dT}{M_i(T_2 - T_1)} = \frac{a_i}{M_i} + \frac{b_i}{2M_i}(T_1 + T_2) \quad (8)$$

$$\bar{u}_b = a_b + \bar{C}_{vb}\, T_b \quad (9a)$$

$$\bar{u}_u = a_u + \bar{C}_{vu}\, T_u \quad (9b)$$

From Equation (9a) the mean burned gases energy derived is expressed in Equation (10), while the mean burn gases energy expressed in terms of the mean burn gases temperature is given by Equation (11).

$$\langle\bar{u}_b\rangle = \int_0^\alpha [a_b + \bar{C}_{vb}\, T_b(\alpha, \alpha')]\, d\alpha' \quad (10)$$

$$\langle\bar{u}_b\rangle = a_b + \bar{C}_{vb}\langle T_b\rangle \quad (11)$$

Where,

$$\langle T_b\rangle = \int_0^\alpha T_b(\alpha, \alpha')\, d\alpha' \quad (12)$$

Substituting Equations (5), (9) and (11) into the energy equation yields the relationship in Equation (13).

$$\frac{d}{d\theta}[m(1-\alpha)(a_u + \bar{C}_{vu}T_u) + m\alpha(a_b + \bar{C}_{vb}\langle T_b\rangle)] = \frac{dQ}{d\theta} - P\frac{dV}{d\theta} \quad (13)$$

Temperature of the unburn gases throughout the combustion cycle can be determined by Equation (14);

$$T_u(\theta) = Pi\left[\frac{P(\theta)}{Pi}\right]^{(\gamma_u - 1)/\gamma_u} \quad (14)$$

To eliminate the burned gas temperature from the energy equation, the relationship in Equation (15) can be employed;

$$\frac{d}{d\theta}\left[m(1-\alpha)a_u + m(1-\alpha)\left(\frac{\gamma_b - \gamma_u}{\gamma_b - 1}\right)\bar{C}_{vu}T_u + m\alpha a_b + \frac{pV}{\gamma_b - 1}\right] = \frac{dQ}{d\theta} - P\frac{dV}{d\theta} \quad (15)$$

Mass fraction of burned gas mixture in the cylinder is given by Equation (16) [25];

$$MFB_\theta = \frac{\sum_{i=ign}^{i=0}\Delta P_{c,i}}{\sum_{i=ign}^{i=N}\Delta P_{c,i}} \quad (16)$$

Where, MFB_θ is the Mass fraction of burned gas mixture at crank angle θ, ΔP_c is the corrected pressure rise due to combustion, *i* is the integer crank angle location, *ign* is the ignition crank angle. Substituting Equation (14) into Equation (15) and differentiating yields the relationship in Equation (17) [21];

$$m(1-\alpha)\left(\frac{\gamma_b-\gamma_u}{\gamma_b-1}\right)\bar{C}_{vu}\,T_i\left(\frac{p}{p_i}\right)^{(\gamma_u-1)/\gamma_u}\frac{1}{p}\frac{\gamma_u-1}{\gamma_u}\frac{dp}{d\theta}+m\left[a_b-a_u-\left(\frac{\gamma_b-\gamma_u}{\gamma_b-1}\right)\bar{C}_{vu}\,T_i\left(\frac{p}{p_i}\right)^{(\gamma_u-1)/\gamma_u}\right]\frac{d\alpha}{d\theta}+\frac{p}{\gamma_b-1}\frac{dV}{d\theta}+\frac{V}{\gamma_b-1}\frac{dp}{d\theta}=\frac{dQ}{d\theta}-P\frac{dV}{d\theta} \quad (17)$$

Equation (17) can be rearranged to show the rate of change of the cylinder pressure in terms of the intake stroke end conditions, rate of volume change as well as the combustion and heat transfer rates in Equation (18);

$$\frac{dp}{d\theta}=\frac{\frac{dQ}{d\theta}-\frac{\gamma_b}{\gamma_b-1}P\frac{dV}{d\theta}-m\left[a_b-a_u-\left(\frac{\gamma_b-\gamma_u}{\gamma_b-1}\right)\bar{C}_{vu}\,T_i\left(\frac{P}{P_i}\right)^{(\gamma_u-1)/\gamma_u}\right]\frac{d\alpha}{d\theta}}{m(1-\alpha)\bar{C}_{vu}\frac{\gamma_b-\gamma_u}{\gamma_b-1}\frac{\gamma_u-1}{\gamma_u}\frac{T_i}{P}\left(\frac{P}{P_i}\right)^{(\gamma_u-1)/\gamma_u}+\frac{V}{\gamma_b-1}} \quad (18)$$

The gas force is the product of the maximum pressure and area of the cylinder given by Equation (19) while the average gas temperature during compression and expansion of the combusted gases is given by Equation (20) [26];

$$F_g = P_{max}\frac{\pi B^2}{4} \quad (19)$$

$$T = T_M\frac{pV}{p_M V_M}\frac{G_M R_M}{GR} \quad (20)$$

Where, p is the cylinder gas pressure, V is the cylinder volume, G is the cylinder gas weight, R is the gas constant.

4. RESULTS AND DISCUSSION

Gasoline contains a number of hydrocarbon compounds which react differently with one another under high temperature-high pressure combustion in the combustion chamber of internal combustion engine due to the number of hydrogen and carbon atoms present, and the bonding pattern of these atoms. The Hydrocarbons (HC) content within the gasoline fuels inside the combustion chamber may not burn easily or may not burn at all except they react with air. This is where the principles behind the chemistry of combustion comes into play. The air which enters the combustion chamber is composed of about 21% Oxygen (O_2), 78% Nitrogen (N_2) and trace quantities of other inert gases including Argon (Ar), Hydrogen (H_2), Carbon dioxide (CO_2), Nitrogen oxide (NO_X), Sulfur dioxide (SO_2) etc. During combustion process, the HC present in the fuel mixture reacts primarily with oxygen to form water vapour (H_2O) and CO_2, giving off heat and pressure within the combustion chamber. A mixture which contains excess air is known as lean or weak mixture while the mixture which has a deficiency of air is referred to as rich mixture. However, a mixture that contains sufficient oxygen for complete combustion of fuel is known as stoichiometric mixture. In other words, the ratio of air to fuel mixture in IC engines play a vital role in the efficiency of combustion cycles. For optimum engine performance, fuel economy and adequate emissions, air-fuel ratio of about 14.7 pound of air for every one pound of fuel is required as the ideal ratio necessary for these conditions. As mentioned earlier, the ideal air-fuel ratio is known as stoichiometry, and is the targeted ratio for the feedback fuel control system. Fuel consumption and emissions are prone to increase with air-fuel ratios richer than stoichiometry, but on the other hand, emissions, power and driving comfort are at the expense with air-fuel ratios leaner than stoichiometry. To determine the air-fuel mix ratio in this case, referenced boundary conditions selected from Solidworks flow regime in Table 2 as well as the engine specifications in Table 1 were employed in the combustion process simulation, and air-fuel mixture ratio of 14.4:1 was obtained. In this case, the 14.4 can also be obtained by dividing 100 by 6.9 (percentage of gasoline fuel by mass in Table 2). The maximum and minimum results obtained as the combusted gas properties for the combustion process simulation is show in Table 3.

In addition to the results presented in Table 3, pressure of the flame trajectories and Temperature flow trajectores of combusted gas in the combustion chamber was further simulated as shown in Figure 2. During combustion, the in-cylinder adiabatic flame temperature for a lean mixture is given by Equation (21) while that of a rich mixture is given by Equation (22);

$$T_R \cong T_0+\frac{m_f.LHV+(m_a+m_f)\bar{C}_{p,R}(T_R-T_0)}{(m_a+m_f)\bar{C}_{p,P}} \quad (21a)$$

$$T_R+\frac{m_f.LHV}{(m_a+m_f)\bar{C}_{p,P}}=T_R+\frac{m_f/m_a.LHV}{(1+m_f/m_a)\bar{C}_{p,P}} \quad (21b)$$

$$T_R+\frac{f.LHV}{(1+f)\bar{C}_{p,P}}=T_R+\frac{\emptyset.f_S.LHV}{(1+\emptyset.f_S)\bar{C}_{p,P}} \quad (21c)$$

$$T_P=T_R+\frac{f.LHV}{(1+f)\bar{C}_{p,P}}=T_R+\frac{f_S.LHV}{(1+\emptyset.f_S)\bar{C}_{p,P}} \quad (22)$$

Where, *mf* and *ma* is the mass of fuel and air, $\bar{C}_{p,P}$ is an average value of specific heat evaluated at the average temperature of reactants and standard temperature, f_S is the stoichiometric fuel/air ratio by mass, T_P is the adiabatic flame temperature.

The combustion flame can be characterized based on the gas flow characteristics in the combustion chamber. The flame resulting from combusted gas in the combustion chamber can either be laminar (stream lined flow) or turbulent (vortex motion). It can be classified as steady or unsteady depending on whether or not the flow pattern or overall motion of the flame changes with time. This agrees with the findings of Pradhan et al. [27], where it was experimentally determined that the flame in an IC engine cycle is characterized by turbulent and unsteady patterns upon the entry of premixed air-fuel mixture into combustion chamber. The presence of turbulent regime in the flame pressure aids in propagating the flame temperature and the flame velocity which in turn accelerate the rate of thermal reaction in the combustion chamber. Converting the 6.9% fuel of gasoline by mass in Table 2, 14.4 ratio by mass was obtained as the air-fuel mixture. Using a mix ratio that is slightly below stoichiometry (such as 14.4:1), hydrocarbon would react with oxygen to produce water vapour (H_2O) and carbon dioxide (CO_2) while Nitrogen (N_2) would pass through the engine without being affected by the combustion process. Given by Equation (23), the balanced chemical equation for such reaction may be expressed as [11];

$$2C_8H_{18}N_2 + 25O_2 \rightarrow 16CO_2 + 18H_2O + 2N_2 \qquad (23)$$

However, combustion stoichiometry for general hydrocarbon fuel, $C_\alpha H_\beta O_\gamma$ with air is given by the following chemical equation;

$$C_\propto H_\beta O_\gamma + \left(\alpha + \frac{\beta}{4} - \frac{\gamma}{2}\right)(O_2 + 3.76N_2) \rightarrow \alpha CO_2 + \frac{\beta}{2}H_2O + 3.76\left(\alpha + \frac{\beta}{4} - \frac{\gamma}{2}\right)N_2 \qquad (24)$$

The power cycle of two stroke internal combustion engine is completed with two strokes which are the upward and downward movement of the piston during one crankshaft revolution. In other words, the end of the combustion stroke and the beginning of the compression stroke occurs simultaneously with the intake and exhaust operation taking place at the same time. According to Mehrnoosh *et al.* [28], the quantitative representations of the flow field during compression consist of swirl and tumble numbers, and in some studies, fluctuation from the cycle mean. During the downward stroke where the reciprocating piston travels downward from Top Dead Center (TDC) to Bottom Dead Center (BDC) as shown in Figure 3, the vacuum created in the cylinder is filled by fresh air entering the combustion chamber through the crankcase.

As the reciprocating piston moves downward, the poppet valve is forced close due to increased crankcase pressure buildup. As shown in Figure 4, the compressed air-fuel mixture gets expanded in the crankcase prior to the end of the stroke. The reciprocating piston traveling towards the end of the stroke exposes the intake port, thereby, allowing the expanded air-fuel mixture to escape into the main cylinder for further combustion and expansion at high temperature and pressure before being expelled out of the exhaust port outside the cylinder.

During the upward stroke where the reciprocating piston travels upward from BDC to TDC due to the fly wheel gaining momentum, the expanded air-fuel mixture in the cylinder/combustion chamber gets ignited by spark plugs at the top of the stroke. Thus, the burning fuel continues to expand, pushing the reciprocating piston downward to complete the cycle. At this point, water vapor, carbon dioxide, nitrogen and other unwanted pollutants are expelled from the cylinder into the exhaust system. Under certain engine operating conditions, Carbon monoxide (CO) which is a by-product of incomplete combustion is formed. This may be due to insufficient oxygen content in the air-fuel mixture during combustion to adequately oxidize the carbon atoms present in the mixture into CO_2. Therefore, the IC engine is prone to oxygen starved combustion process when it operates with air-fuel ratios richer than stoichiometry (14.7), and excessive CO emission may be caused by leaky injectors, improper closed loop controls, high fuel pressure etc. during cold operation, warm up and power enrichment, whereas, very little amount of CO is emitted when the engine is at warm idle or cruise mode because of sufficient oxygen content in the air-fuel mixture to oxidize the carbon atoms. This results in the emission of excess CO_2, the ideal by-product of complete combustion process. Despite the technological advancement in automotive applications, automobile engines under certain operating conditions still emit some level of harmful emissions. For example, high cylinder temperature and pressure combustion (typically during heavy loading conditions) within the cylinder can result in the reaction of nitrogen with oxygen to form Oxides of Nitrogen (NO_X) which is primarily composed of 98% nitric oxide (NO). The major causes of excessive NO_X emission from the engine may include lean air-fuel mixture, faulty Exhaust Gas Recirculation (EGR) system operation, high temperature air intake overheated engine etc. Figure 5 shows the temperature variation (0-3000ºC) of the expanded gases in the cylinder while Figure 6 illustrates the flow trajectory of the combusted gas pressure (0-80 bar) in the cylinder. Using the engine specifications and boundary conditions in Table 1 and 2 to simulate the engine operation cycle with air-fuel mixture ratio of 14.4:1, the following reactant and product gases are summarised in Table 4.

Figure 7 represents a plot of combusted gas temperature against time. This indicates that the temperature of air entering the cylinder is about 293.92 K, but increases significantly to about 3000 K during the high temperature-high pressure combustion of HC, and decreases again as fresh air enters the cylinder. Similarly in Figure 8, velocity of the combusted gases rises and falls corresponding to the high temperature-high pressure air-fuel combustion in the combustion chamber.

Figure 9 shows the plot of dynamic viscosity against temperature of combusted gases. It can be observed from the plot that the dynamic viscosity of the combusted gas increases as the combustion temperature increases. This is in agreement with the findings of Jennings et al. [29], where the relationship between temperature and dynamic viscosity of gas was experimentally determined in gas chromatography. Plot of specific heat against temperature of combusted gas is presented in Figure 10. An increasing gas temperature from 0-2000 K at a constant specific heat of 1000 J/kg*k can be observed, while the specific heat begins to increase from 1000 J/kg*k as the temperature continues to increase. For example, when gas is heated at a constant volume like in the case of the combustion chamber, heat energy within the volume raises the temperature as well as the gas internal energy. This is because in a controlled volume, the gas cannot expand further beyond the containment. The relationship between thermal conductivity and temperature of the combusted gas is presented in Figure 11. With respect to the temperature dependency on the thermal conductivity of the combusted gas, it is observed that entities increase in proportion with one another. The conduction of heat by gas occurs through particle collision. That is, gas particles in a region of higher temperature will possess a higher mean velocity of their random motion. Therefore, upon collision of the gas particles in nearby region, their momentum entangles, leading to propagation of heat/energy in the gas.

Table 3: Properties of Simulated In-cylinder Combusted Gas

Property	Minimum	Maximum
Pressure [bar]	60.76	80.20
Temperature [K]	293.92	3000.60
Density (Fluid) [kg/m^3]	7.49	75.40
Velocity [m/s]	0	74.967
Velocity (X) [m/s]	-28.039	34.668
Velocity (Y) [m/s]	-47.943	74.756
Velocity (Z) [m/s]	-36.431	36.642
Temperature (gas mixture) [K]	298.00	3000.60
Temperature (Solid walls) [K]	293.92	2367.56
Density (Solid) [kg/m^3]	2800.00	8000.00
Mach Number	0	0.08
Vorticity [1/s]	0.947	52089.452
Shear Stress [bar]	0	1.76e-003
Relative Pressure [bar]	62.76	80.20
Prandtl Number	0.6370804	0.7097623
Heat Transfer Coefficient [W/m^2/K]	0.148	581.238
Surface Heat Flux [W/m^2]	-9696983.012	3392631.823
Heat Flux [W/m^2]	36.385	3.783e+007
Overheat above Melting Temperature [K]	-3.403e+038	-3.403e+038

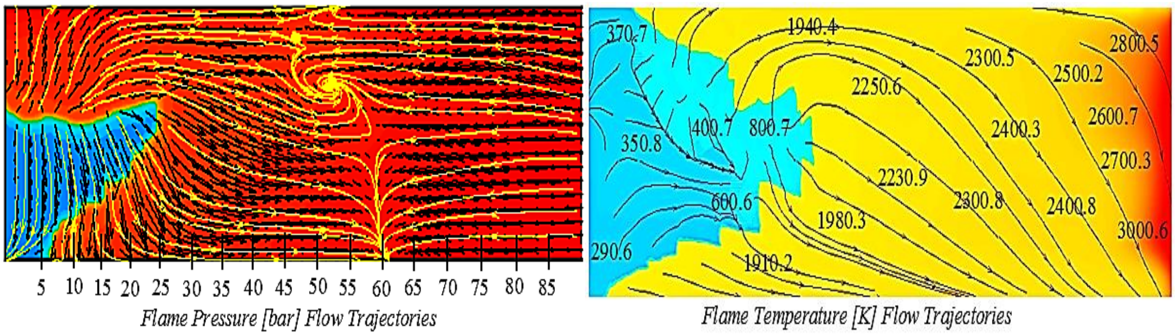

Fig. 2: Pressure of the flame trajectory and Temperature flow trajectory of combusted gases

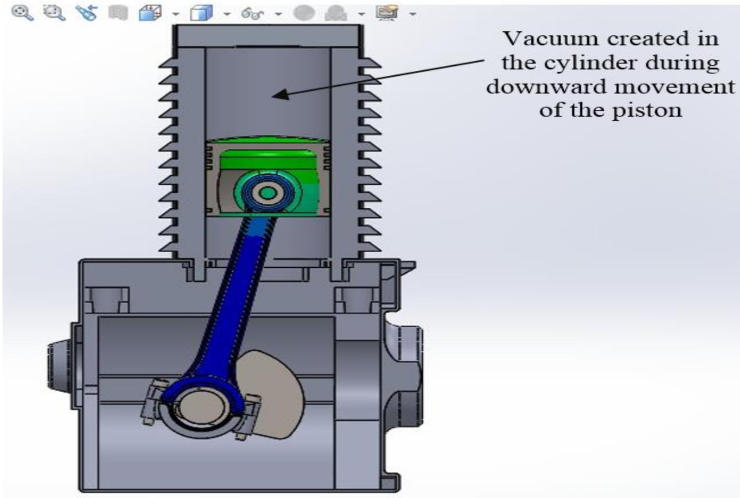

Fig. 3: Surface Plot showing downward movement of the Piston and connecting Rod

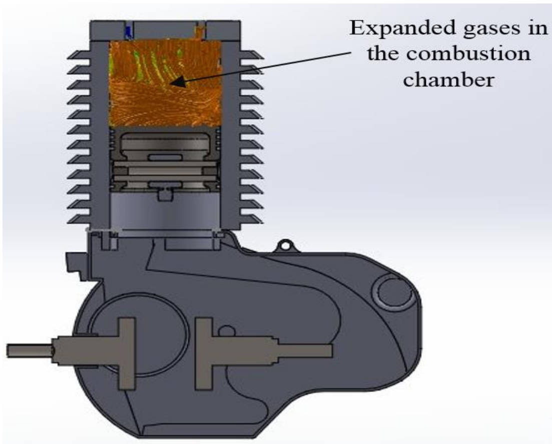

Fig. 4: Flow Trajectory showing expanded Gases in the Combustion Chamber

Table 4: Summary of Combusted Gases at Air-fuel Mixture of 14.4:1

Intake and Compression Stroke	Power and Exhaust Stroke
Reactant	Products
26% Oxygen (O_2)	3.2% Water vapor (Steam) (H_2O)
73 % Nitrogen (N_2)	96.2% Carbon dioxide (CO_2)
1 mole Hydrocarbon HC	0.6% Nitrogen (N_2)

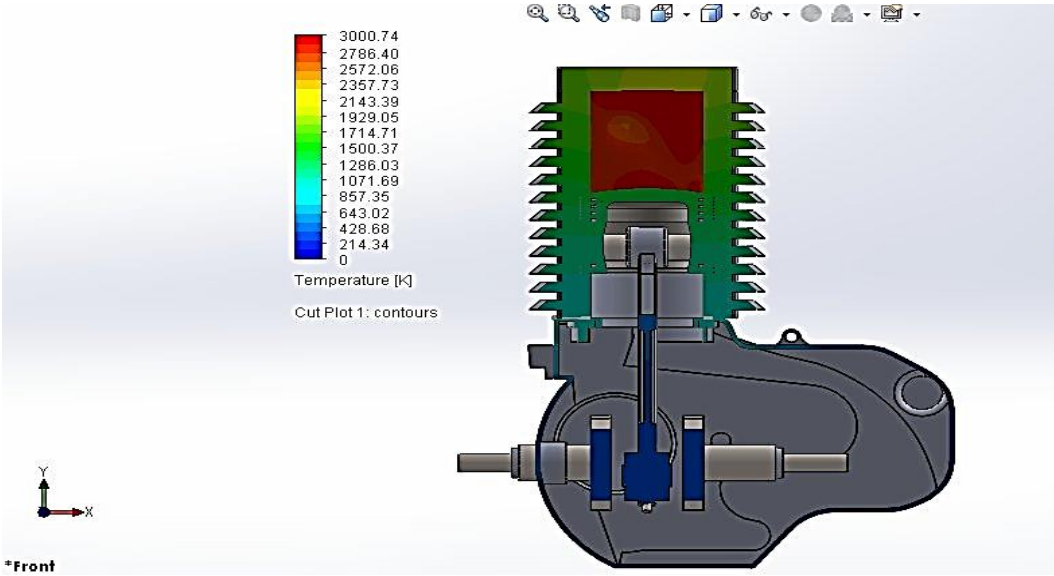

Fig. 5: Temperature variation of the expanded gases in the cylinder

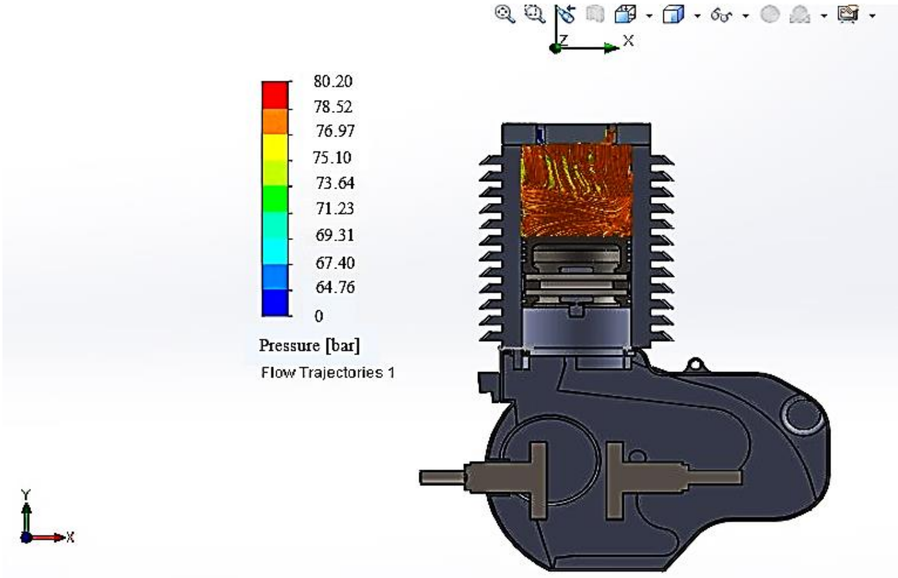

Fig. 6: Flow Trajectories of the Combusted Gas Pressure in the Combustion Chamber

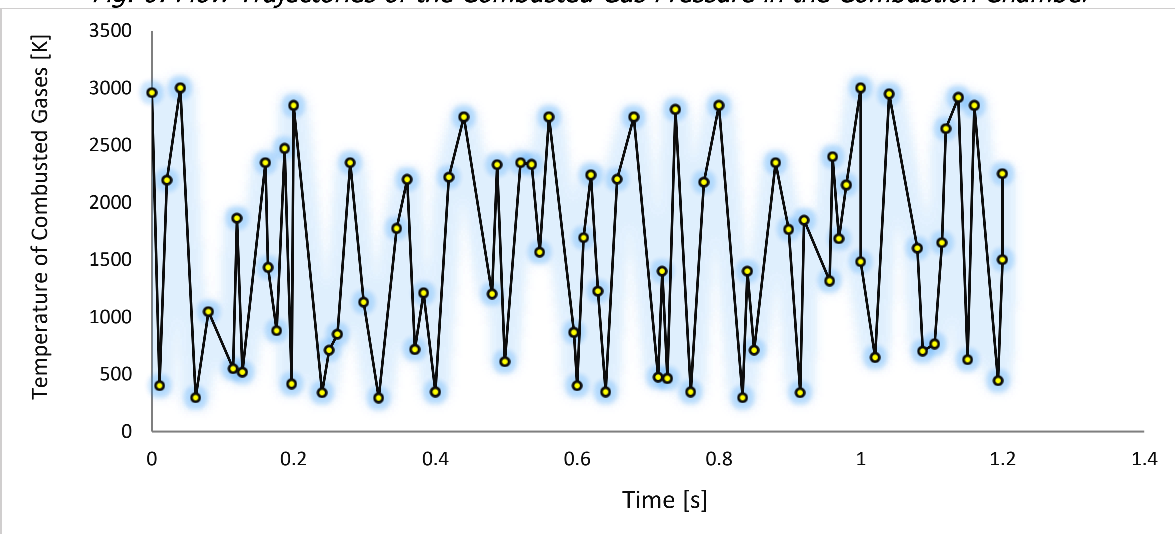

Fig. 7: Plot of Temperature of Combusted Gases against Time

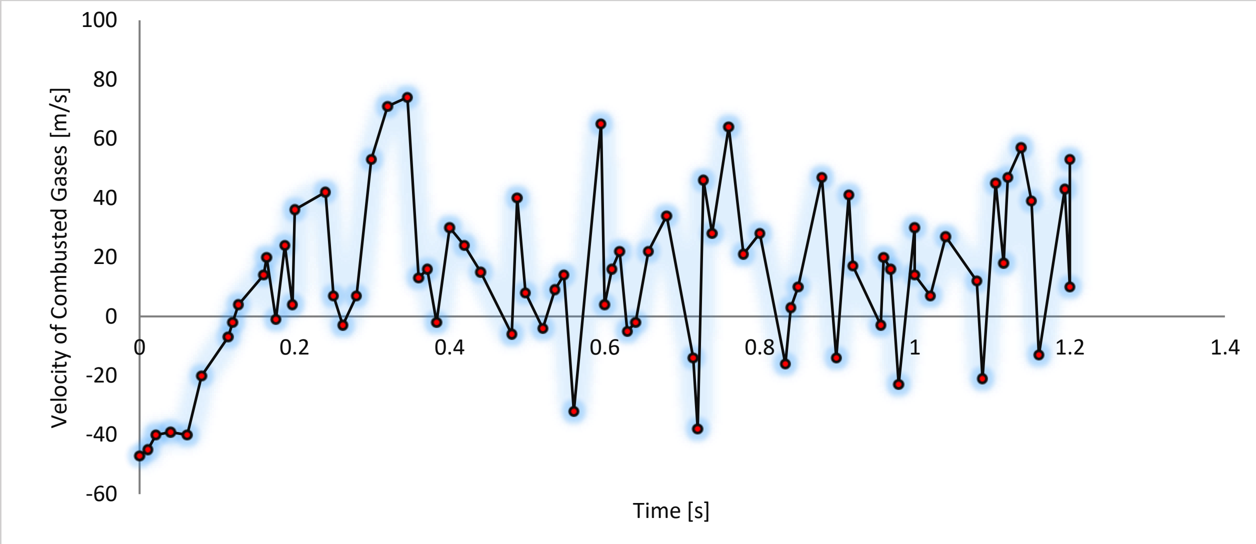

Fig. 8: Plot of Velocity of Combusted Gases against Time

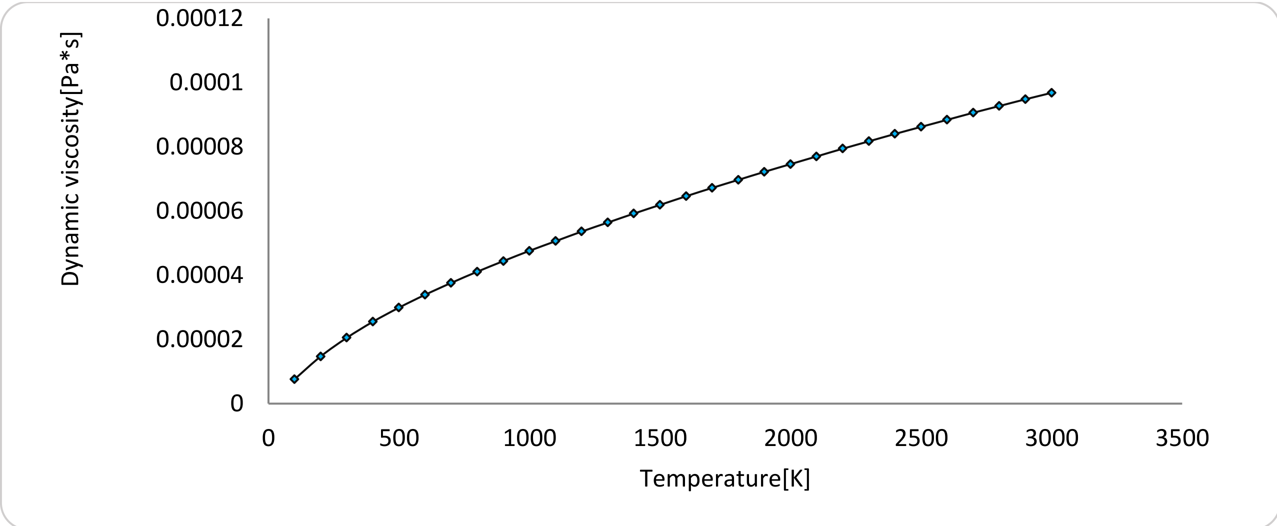

Fig. 9: Plot of Dynamic Viscosity against Temperature of Combusted Gas

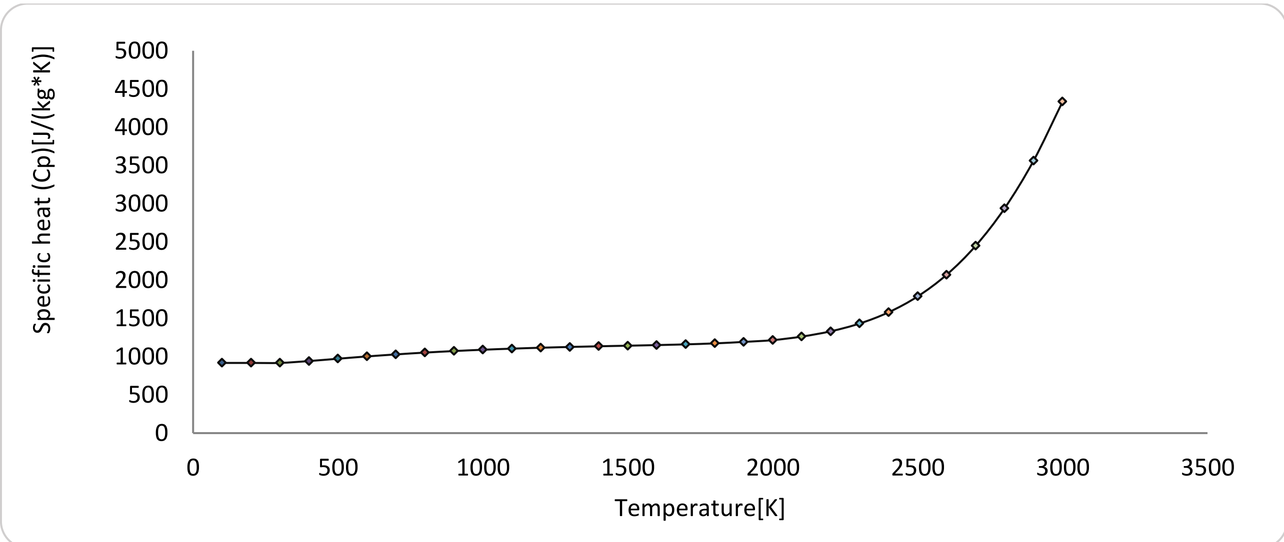

Fig. 10: Plot of Specific Heat against Temperature of Combusted Gas

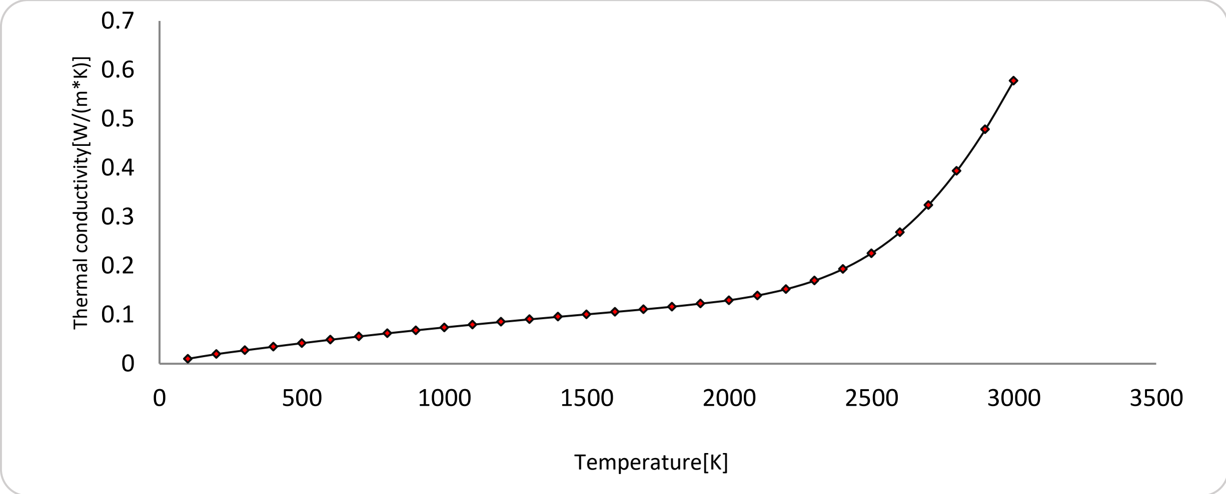

Fig. 11: Plot of Thermal Conductivity against Temperature of Combusted Gas

5. CONCLUSION

The gas dynamics inside the cylinder of two stroke internal combustion engine in its service condition which is characterized by thermodynamic properties such as temperature, velocity, dynamic viscosity, specific heat and velocity was modelled in this study. It was observed that the inability of the engine to perform under adequate air-fuel mixture of 14.1:7 would result in undesired conditions such as incomplete combustion of the in-cylinder gases due to limited supply of oxygen while intensively high temperature and pressure, for example above the 3000K obtained in this study can lead to the formation and emission of nitrogen oxides (NO_X) which primarily consists of nitric oxide (NO). With an air-fuel mixture ratio of 14.4:1 which was gotten from preliminary simulation of the boundary conditions with the engine specifications adequately maintained, combusted products of 96.2% CO_2, 3.2% H_2O and 0.6% N_2 was obtained. This implies that an air-fuel ratio of 14.4:1 which shows proximity with stoichiometric ratio can still yield CO_2 as the principal by product of efficient combustion in two stroke engine cycle.

6. REFERENCES

[1]. Caton, J. A. (2018) The Thermodynamics of Internal Combustion Engines: Examples of Insight. *Inventions,* 3(33), 1-30.

[2]. Ikpe A. E., Owunna, I., Ebunilo, P. O. and Ikpe, E. (2016a) Material Selection for High Pressure (HP) Compressor Blade of an Aircraft Engine. *International Journal of Advanced Materials Research,* 2(4), 59-65.

[3]. Ikpe A. E., Owunna, I., Ebunilo, P. O. and Ikpe, E. (2016b) Material Selection for High Pressure (HP) Turbine Blade of Conventional Turbojet Engines. *American Journal of Mechanical and Industrial Engineering,* 1(1), 1-9.

[4]. Lewis, D. (2013) A Quasi-Dimensional Spark Ignition Two Stroke Engine Model. Loughborough University.

[5]. Soda, M. (2013) Numerical Investigation of Internal Combustion Engine Related Flow. KTH Mechanics, SE-100 44 Stockholm, Royal Institute of Technology, Sweden.

[6]. Kosenok, B. S., Balyakin, V. B. and Giltsov, I. N. (2017) The use of Vector Models to Study the Dynamic Characteristics of An Advanced Two-Shaft Internal Combustion Engine. *Procedia Engineering,* 176, 37-42.

[7]. Rakopoulos, C. D. and Giakoumis, E. G. (2006) Second-law Analysis Applied to Internal Combustion Engines Operation. *Progress in Energy and Combustion Science,* 32, 2-47.

[8]. Duygu, I. and Halit, K. (2016) Dynamic and Thermodynamic Examination of a Two-stroke Internal Combustion Engine. *Politeknik Dergisi,* 19(2), 141-154.

[9]. Blair G. P. (1996) Design and Simulation of Two-Stroke Engines, U.S.A: Society of Automotive Engineers, Inc.

[10]. Cantore G., Mattarelli E., Rinaldini C.A., (2014) A new design concept for 2-Stroke aircraft Diesel engines. *Energy Procedia,* 45, 739-748.

[11]. Eastop, T. D. and McConkey, A. (1993) Applied Thermodynamics for Engineering Technologies. Pearson Education Ltd, ISBN 978-81-7758-238-3.

[12]. Pulkrabek, W. P. (2003) Engineering Fundamental of the Internal Combustion Engine (2nd Edition), Pearson publishers, ISBN-13: 978-0131405707.

[13]. Rajput, R. K. (2007) A Text Book of Engineering Thermodynamics, Laxmi Publication, ISBN: 13: 978-813180058X.

[14]. Amin M. A., Azhar A. A., MohdF. M. S., Zulkarnain A. L. (2014) An experimental study on the influence of EGR rate and fuel octane number on the combustion characteristics of a CAI two-stroke cycle engine. *Applied Thermal Engineering,* 71: 248-258.

[15]. Pradeep V., Bakshi S., Ramesh A. (2014) Scavenging port based injection strategies for an LPG fuelled two-stroke spark-ignition engine, *Applied Thermal Engineering,* 67, 80-88.

[16]. Volckens J., Olson D. A., Hays M. D. (2014) Carbonaceous species emitted from hand held two-stroke engines, *Energy Procedia,* 45, 739-748.

[17]. Quintero H.F., Romero C. A., Useche L. V. V. (2007) Thermodynamic and dynamic of an internal combustion engine with a noncircular-gear based modified crank-slider mechanism. 12th IFToMM World Congress, Besançon (France) 1-6, (2007).

[18]. Zhang, G. Q. and Assanis, D. N. (2003) Manifold Gas Dynamics Modelling and Its Coupling with Single-Cylinder Engine Models Using Simulink. *Journal of Engineering for Gas Turbines and Power,* 125, 563-571.

[19]. Andwari, A. M., Aziz, A. A., Said, M. F. M., and Latiff, Z. A. (2013) Controlled Auto-Ignition Combustion in a Two-Stroke Cycle Engine Using Hot Burned Gases. *Applied Mechanics and Materials,* 388, 201-205.

[20]. Sharavanan, R. and Ezhil, V. M. (2017) Performance Analysis of High Efficiency Petrol Engine. *International Journal of Pure and Applied Mathematics,* 116(14), 517-523.

[21]. Ramachandran, S. (2009) Rapid Thermodynamic Simulation Model of an Internal Combustion Engine on Alternate Fuels. Proceedings of the International Multi-conference of Engineers and Computer Scientists, Hong Kong, 2, 18-20.

[22]. Ferguson, C. R. and Kirkpatrick, A. T. (2000) Internal Combustion Engine: Applied Thermosciences, 2nd Edition, New York, John Willey and Sons, ISBN: 0471356174.

[23]. Edwards, K. D., Wagner, R. M., Briggs, T. E., Tim, J., Singh, G. and Gemmer, B. (2011) Defining Engine Efficiency Limits. 17th DEER Conference, 3-6 October, Detroit, MI, USA.

[24]. Ganesan, V. (2013) Internal Combustion Engine, 4th Edition. Tata McGraw-Hill Education Pvt. Ltd, USA, ISBN: 13: 9781259006197.

[25]. Ceviz, M. A. and Kaymaz, I. (2005) Temperature and Air-fuel Ratio Dependent Specific Heat Rati Functions for Lean Burned and Unburned Mixture. *Energy Conversion and Management,* 46, 2387-2404.

[26]. Nigus, H. (2015) Kinematics and Load Formulation of Engine Crank Mechanism. Mechanics, Materials Science and Engineering, ISSN: 2412-5954.

[27]. Pradhan, R., Ramkumar, P., Sreenivasan, M. and Sukumar, P. (2012) Air-fuel Ratio (Afr) Calculation in an Internal Combustion Engine Based on the Cylinder Pressure Measurements. *International Journal of Engineering Research and Application,* 2(6), 1378-1385.

[28]. Mehrnoosh, D., Asghar, H. A. and Asghar, M. A. (2012) Thermodynamic Model for Prediction of Performance and Emission Characteristics of SI Engine Fuelled by Gasoline and Natural Gas with Experimental Verification. *Journal of Mechanical Science and Technology,* 26(7), 2213-2225.

[29]. Jennings, W., Mittlefehldt, E. and Stremple, P. (1997) Analytical Gas Chromatography, 2nd Edition, Elsevier Inc, ISBN: 978-0-12-384357-9.